ISSN 0001-4338, Izvestiya, Atmospheric and Oceanic Physics, 2023, Vol. 59, No. 9, pp. 1208–1219. © Pleiades Publishing, Ltd., 2023.
Russian Text © The Author(s), 2023, published in Issledovanie Zemli iz Kosmosa, 2023, No. 3, pp. 81–96.

PHYSICAL BASES AND METHODS OF STUDYING THE EARTH FROM SPACE

Dielectric Model of the Upper Organic Layer of Forest Soils for a Frequency of 435 MHz

A. Yu. Karavaiskii[a], * and Yu. I. Lukin[a]

[a] *Kirensky Institute of Physics, Siberian Branch, Russian Academy of Sciences, Krasnoyarsk, 660036 Russia*

**e-mail: rsdak@ksc.krasn.ru*

Received June 28, 2022

Abstract—A dielectric model based on the refractive dielectric model of the mixture of thawed and frozen forest organic soils in the root zone for a frequency of 435 MHz has been developed. The model is created on the basis of dielectric measurements of four soils whose organic matter content varies in the range from 15 to 31%. The dielectric measurements are carried out in the range of the gravimetric moisture from 0 to 0.6 g/g and temperature range from –30 to 25°C. The coefficient of determination (R^2) between values calculated by the model and measured values of the real (ε') and imaginary (ε'') parts of complex dielectric permittivity is 0.97. The normalized root-mean-square error is 16 and 21% for the real and imaginary parts of the complex dielectric permittivity, respectively. This dielectric model may be applied in remote sensing algorithms when retrieving the value of forest soil moisture in the root zone from radar and radiometric data.

Keywords: dielectric model, moisture, temperature, organic soil, frozen soil, thawed soil

DOI: 10.1134/S0001433823090104

INTRODUCTION

The root zone of forest soils is critical for the regulation of the soil, water, and mineral–organic balance necessary for forest ecosystem functioning (Shukla and Mintz, 1982). Moisture of the active layer of forest soils is an important variable for applications in hydrology, agriculture, meteorology, and climate changes (Garrison et al., 2017; Nagarajan et al., 2012; Sabater et al., 2007).

At present, spaceborne radiometric methods for measuring the moisture in the topsoil with a thickness of up to 5 cm in the global scale based on data from the Soil Moisture and Ocean Salinity (SMOS) (Kerr et al., 2010; Pan et al., 2012) and Soil Moisture Active Passive) (SMAP (Entekhabi et al., 2010; Pan et al., 2016) satellites in the L-band frequency range (1.4 GHz) are developed (Escorihuela et al., 2010; Monerris et al., 2006). For soils covered by thin vegetation, the error in measurements of the volume water content by radiometric methods is about 4% (Grant et al., 2010; Zhang et al., 2011). To increase the depth of soil moisture monitoring, research on the development of remote sensing techniques in the P-band frequency range has been carried out in recent years (Reigber et al., 2012; Garrison et al., 2017; Alemohammad et al., 2018; Carreiras et al., 2017). It has been shown that the depth of moisture sensing at a frequency of 750 MHz with the use of a ground-based polarimetric radiometer (the observation angle of 30°) for soil not covered by vegetation can reach ~7–10 cm (Ye et al., 2020; Shen et al., 2021). In the course of airborne radar polarimetric observations at a frequency of 435 MHz, the possibility of retrieving the vertical soil moisture distribution to a depth of about several tens of centimeters was demonstrated (Tabatabaeenejad et al., 2015). The European Space Agency plans to launch the BIOMAS satellite equipped with a synthesized aperture radar with an operation frequency of 435 MHz (P-band) (Alemohammad et al., 2018; Carreiras et al., 2017), which creates a technological capability of remote sensing of soil moisture under thick vegetation, including the forest canopy (Jagdhuber et al., 2012).

In this aspect, models of complex dielectric permittivity (CDP) of soils are one of the main elements in algorithms for retrieving soil moisture from radar and radiometric observations with the use of physical models of radar scattering and thermal radio radiation. Until now, no generalized dielectric model has been created in the P-band frequency range (435 MHz) for forest soils whose active layer has a considerable gradient of the organic matter content (Liebmann et al., 2020).

There are a number of classical models that describe properties of dispersed systems and include in some way or another dielectric permittivities of the substances constituting them: the Lichtenecker, Bruggeman–Hanai, Brown, and Odelevskii models (Shutko, 1986). A comparison of calculation results obtained when using three-component models (mineral–water–air) with experimental data for samples of sand

and clay with moisture of up to 20% shows that the refractive model of dielectric permittivity of the mixture yields the best coincidence (Shutko, 1986). However, this does not take into account the fact that a portion of moisture is present in soil in the form of bound water. Dielectric permittivity of bound water must be within limits from dielectric permittivity of ice to that of free water depending on the soil moisture content (Wang and Schmugge, 1980; Dobson et al., 1985). In connection with this, it is necessary to take into account the content of bound water and its dielectric permittivity in soil CDP models (Mironov et al., 1994; Boyarskii and Tikhonov, 1995; Boyarskii and Tikhonov, 2003).

In (Mironov et al., 2005), in the frequency range of 0.8–12.5 GHz, the measurement results for CDP of tundra forest soils collected in Tura (East Siberia) were shown. The content of the clay fraction and humus in those soils varied from 3.25% to 24% and from 0.28% to 4%, respectively. The authors of (Mironov et al., 2005) described the CDP of soils using a four-component refractive dielectric model whose parameters were found for each soil sample individually. In (Owe et al., 1998), at a frequency of 1.67 (the L-band) and 5 GHz (the C-band), CDP was measured for a forest soil with the content of the clay fraction and organic matter of 10.5 and 1.47%, respectively. Based on these measurements, it was shown that the Schmugge–Wang model (Wang and Schmugge, 1980) described the dependence of the CDP of soils on the volume water content more accurately as compared to the Dobson model (Dobson et al., 1985). Different authors made attempts to generalize the results of dielectric measurements of a collection of soil samples with a mixed organomineral composition in a wide frequency range using the refractive dielectric model (Mandrygina, 2004, the humus content in the soils is 0.6, 6.6, 8.95, and 100%; Bobrov et al., 2008, the content of the clay fraction and humus is 0.3–12.8% and 4.35–56.1%, respectively; Repin, 2010; Bobrov et al., 2013, the content of the clay fraction and humus is 0.8–72% and 0–6.6%, respectively; and Belyaeva et al., 2013; Liu et al., 2013, the content of the clay fraction and organic matter from 6.7 to 68.7% and from 3 to 17.8%, respectively), as well as with the use of other models of mixture CDP (Park et al., 2017, 2019). Due to the influence of Maxwell–Wagner relaxation processes caused by polarization of water–mineral and water–air phase interfaces, the highest accuracy of describing experimental CDP values in the ultrawide frequency range from 1 kHz to 20 GHz is achieved when using a combination of the Cole–Cole multirelaxation model (Szypłowska et al., 2021) and the refractive model (Bobrov et al., 2022). As shown in (Repin, 2010), using the Cole–Cole multirelaxation model for describing the CDP of tightly bound water yields a higher accuracy than using the Debye model. When using a combined multirelaxation dielectric model, parameters are selected for each soil type individually, and attempts to obtain general dependences on the content of the clay fraction and humus for all model parameters are unsuccessful (Bobrov et al., 2022). For example, previously, the authors of (Mandrygina, 2004; Bobrov et al., 2008; Liu et al., 2013) attempted to obtain a generalized formula for a quantitative estimate of the maximum content of bound soil water as a function of the content of clay and organic matter (humus). However, such generalized dependences have a low correlation between measured values of the maximum content of bound soil water and corresponding values calculated by the model when comparing with a set of independent data (Bobrov et al., 2008).

At the same time, it has been shown that a modification of the refractive model with allowance for local particularities in the content of the clay fraction and humus in soils of sparse forests of northern China allows one to improve the accuracy of retrieving the soil moisture approximately twofold: from 30 to 13% and from 16 to 7%, respectively, when using radiometric data from the SMAP and SMOS satellites at a frequency of 1.4 GHz (Jin et al., 2017). For the operation frequency of radiometers onboard the SMAP and SMOS satellites, 1.4 GHz, the CDP was measured and single-frequency specialized models were created for soils rich in organic matter, including soils of boreal forests (Bircher et al., 2016). The authors of (Bircher et al., 2016) showed that CDP values for moist soils with a high content of organic matter were lower than CDP values for moist soils with a high content of the mineral matter, because organic soils contain more bound water than mineral soils; the dielectric permittivity of bound water is less than that of unbound water. Individual specialized dielectric measurements were carried out for forest soils of India at a frequency of 9.6 GHz in the volume water content range from 0 to 30% (Patil et al., 2018), gray forest soils (Chashnikovo, Moscow oblast) containing 11% of soil particles with a size less than 0.001 mm and organic matter of 1.8% at a frequency of 50 MHz (Chudinova, 2009), and peat (Vasyugan Swamp) in a temperature range from –30 to 30°C and in a frequency range from 10 MHz to 40 GHz (Kochetkova, 2019).

At the same time, there are few results in the literature on studying the dielectric properties of organomineral forest soils in P-band frequency ranges (at a frequency of 435 MHz) with the aim of developing specialized dielectric models for using in algorithms of the BIOMAS satellite. Previously, specialized models at the frequency of 435 MHz were developed for mineral (Fomin and Muzalevskiy, 2021) and organic (Savin et al., 2022) thawed and frozen soils, the samples of which were collected in the tundra (Alaska, Yamal Peninsula, and Taimyr Peninsula). Single-frequency models of soil CDP, when compared with spectroscopic models (Mironov et al., 2020; Peplinski et al., 1995; Zhang et al., 2010), possess higher accuracy and have significantly fewer input parameters, which is an advantage in applied remote

1 2 3 4

Fig. 1. Soils under study. The numbers correspond to the numbers of soils from Table 1.

sensing problems in which there is no necessity for information about the finer parameters of the model, such as the CDP of bound water, relaxation time, static dielectric permittivity, entropy and enthalpy of the phase transition, etc. (Bobrov et al., 2021).

In this paper, a single-frequency dielectric model of thawed and frozen organomineral soils collected from the topsoil of mostly pine, birch, and mixed forests of the Krasnoyarsk forest steppe is proposed for using at the frequency of 435 MHz. The dielectric model is created based on the refractive model of a mixture (Komarov and Mironov, 2000; Mironov et al., 2020), the parameters of which are determined depending on the temperature of forest soils.

MATERIALS AND METHODS

The soil samples were collected in the form of cylindrical cores with a diameter of 110 mm and height of 300 mm from the topsoil of the pine, aspen, mixed, and birch forests of the Krasnoyarsk forest steppe, Pirovsky raion, Krasnoyarsk krai. For the modification of the refractive dielectric model, the upper core layer (from 5 to 10 cm) was collected. It mostly contained remains of rotten and not rotten vegetation, fallen leaves, a root system, and a small amount of soil (mostly black) that remained on plant roots (Fig. 1). The coordinates of soils samples and the organic matter content are presented in Table 1. The study was carried out for soil samples with different gravimetric moisture from the dry state to moisture of 0.6 g/g and in the temperature range from −30 to 25°C. The general procedure of preparing the soil samples for measurements was described in detail in (Mironov et al., 2013). The organic matter content in the soil was determined according to GOST 27784-88 and GOST 26213-91; the content of the granulometric composition was determined according to Kachinskii's procedure (Agrochemical..., 1975) (Krasnoyarsk State Center of Agrochemical Service). The determination of the granulometric composition according to Kachinskii's procedure for soils with an organic matter content above 20% turned out to be impossible; for this reason, Table 1 does not contain data on the granulometric composition for such soils.

The gravimetric moisture content of the soil samples m_g was defined as the ratio of the mass of water

Table 1. Organic matter content and granulometric composition of the soils under study

No.	Location coordinates	Forest type	Mass fraction of the organic matter, %	Fraction content, %					
				1–0.25 mm	0.25–0.05 mm	0.05–0.01 mm	0.01–0.005 mm	0.005–0.001 mm	<0.001
1	57°37′17.9″ N 92°13′00.6″ E	Pine	21.4	–	–	–	–	–	–
2	57°37′22.8″ N 92°13′01.4″ E	Aspen	31.1	–	–	–	–	–	–
3	57°37′21.1″ N 92°15′03.0″ E	Mixed	27.8	–	–	–	–	–	–
4	57°39′45.0″ N 92°16′12.2″ E	Birch	14.8	2.8	10.8	47.3	10.5	12.8	15.8

in the soil m_w to the mass of dry soil m_d: $m_g = m_w/m_d$. The error in measurements of moisture varied from 3 to 5% depending on the gravimetric moisture. In total, 20 samples with different moistures were prepared for each soil.

The measurements of CDP of moist samples were carried out using a dielectric measurement complex that included a Keysight N5232 vector network analyzer, an SU-241 Espec temperature chamber, a coaxial measuring container, and a PC. The measured sample of soil with a given moisture was placed in a container made in the form of a rigid coaxial line. Samples with low moisture were measured using a container with a length of 37 mm; samples with high moisture were measured a container with a length of 17 mm. The radius of the outer envelope of both containers was 7 mm; the radius of the central conductor was 3 mm. The measurements were carried out in a temperature range from −30 to 25°C. The stable given temperature of the sample was maintained using an SU-241 Espec temperature chamber. The accuracy of the temperature setting in the chamber is 0.1°C. Using the vector network analyzer, the amplitudes and phases of the scattering matrix element S_{12} of the moist soil samples were recorded at the electromagnetic field frequency of 435 MHz. By means of the technique expounded in (Mironov et al., 2013), using the measured values of the scattering matrix element S_{12}, values of the real and imaginary parts of the complex refractive index (CRI) of moist mineral soil samples $n_s^* = n_s + i\kappa_s$ were obtained, where n_s and κ_s are the refractive index (RI) and the normalized attenuation coefficient (NAC) of the electromagnetic wave in the measured sample, respectively. The technique expounded in (Mironov et al., 2013) allows one to measure CDP with an error from 1 to 10% for the real part and from 6 to 30% for the imaginary part of CDP depending on values of these quantities and electromagnetic field frequency.

The CRI is related to CDP $\varepsilon_s^* = \varepsilon_s' + i\varepsilon_s''$ by the following relationship:

$$n_s^* = \sqrt{\varepsilon_s^*} = \sqrt{\varepsilon_s' + i\varepsilon_s''},$$

where ε_s' is relative dielectric permittivity (DP) of moist soil and ε_s'' is the dielectric loss factor (DL). DP and DL can be easily expressed in terms of the RI and NAC as follows:

$$\varepsilon_s' = n_s^2 - \kappa_s^2, \quad \varepsilon_s'' = 2n_s\kappa_s.$$

SINGLE-FREQUENCY REFRACTIVE DIELECTRIC MODEL

The dependences of soil CDP on moisture, in accordance with (Mironov and Savin, 2019), were described using the dielectric model based on the refractive equation of dielectric permittivity of the mixture. Previously, in (Mironov et al., 2010; Mironov and Savin, 2019), in the studies of organic soils collected in tundra regions, three categories of soil water were identified, namely, tightly bound water, loosely bound water, and unbound water (or ice in frozen soil). This classification was used based on differences in CDP values for categories of water in wet soil. In connection with this, the following refractive dielectric equation of a mixture with three categories of soil water was used for the organic soils under study:

$$\frac{n_s - 1}{\rho_d} = \begin{cases} \dfrac{n_m - 1}{\rho_m} + \dfrac{n_b - 1}{\rho_b} m_g, \quad m_g \le m_{g1}, \\ \dfrac{n_m - 1}{\rho_m} + \dfrac{n_b - 1}{\rho_b} m_{g1} + \dfrac{n_t - 1}{\rho_t}(m_g - m_{g1}), \\ m_{g1} < m_g \le m_{g2}, \\ \dfrac{n_m - 1}{\rho_m} + \dfrac{n_b - 1}{\rho_b} m_{g1} + \dfrac{n_t - 1}{\rho_t}(m_{g2} - m_{g1}) \\ + \dfrac{n_{u,i} - 1}{\rho_{u,i}}(m_g - m_{g2}), \quad m_g > m_{g2}, \end{cases} \tag{1}$$

$$\frac{\kappa_s}{\rho_d} = \begin{cases} \dfrac{\kappa_m}{\rho_m} + \dfrac{\kappa_b}{\rho_b} m_g, \quad m_g \le m_{g1}, \\ \dfrac{\kappa_m}{\rho_m} + \dfrac{\kappa_b}{\rho_b} m_{g1} + \dfrac{\kappa_t}{\rho_t}(m_g - m_{g1}), \\ m_{g1} < m_g \le m_{g2}, \\ \dfrac{\kappa_m}{\rho_m} + \dfrac{\kappa_b}{\rho_b} m_{g1} + \dfrac{\kappa_t}{\rho_t}(m_{g2} - m_{g1}) \\ + \dfrac{\kappa_{u,i}}{\rho_{u,i}}(m_g - m_{g2}), \quad m_g > m_{g2}. \end{cases} \tag{2}$$

The subscripts s, d, m, b, t, u, and i in systems of equations (1) and (2) refer to wet soil, dry soil, organomineral component, tightly bound water, loosely bound water, unbound water, and ice, respectively; m_{g1} is the maximum possible content of tightly bound water in weight in the soil; m_{g2} is the maximum possible content of the total amount of bound water in the soil in weight; m_g is the gravimetric moisture content of the sample; ρ_d is the density of the dry soil; $\rho_{b,t,u}$ are the densities of the soil water categories; and ρ_i is the density of ice. Equations (1) and (2) describe the dependences of the RI and NAC reduced in a certain way to common density of the dry soil on the gravimetric moisture content by piecewise linear functions with breakpoints corresponding to m_{g1} and m_{g2}. An approximation of experimental moisture dependences of the RI and NAC by the use of Eqs. (1) and (2) makes it possible to determine values of m_{g1} and m_{g2} in wet soil at each measurement temperature. As an example, symbols in Fig. 2 show the obtained dependences of reduced RIs $((n_s - 1)/\rho_d)$ and NACs (κ_s/ρ_d) of the soils on moisture at temperatures of 20 and −20°C. As

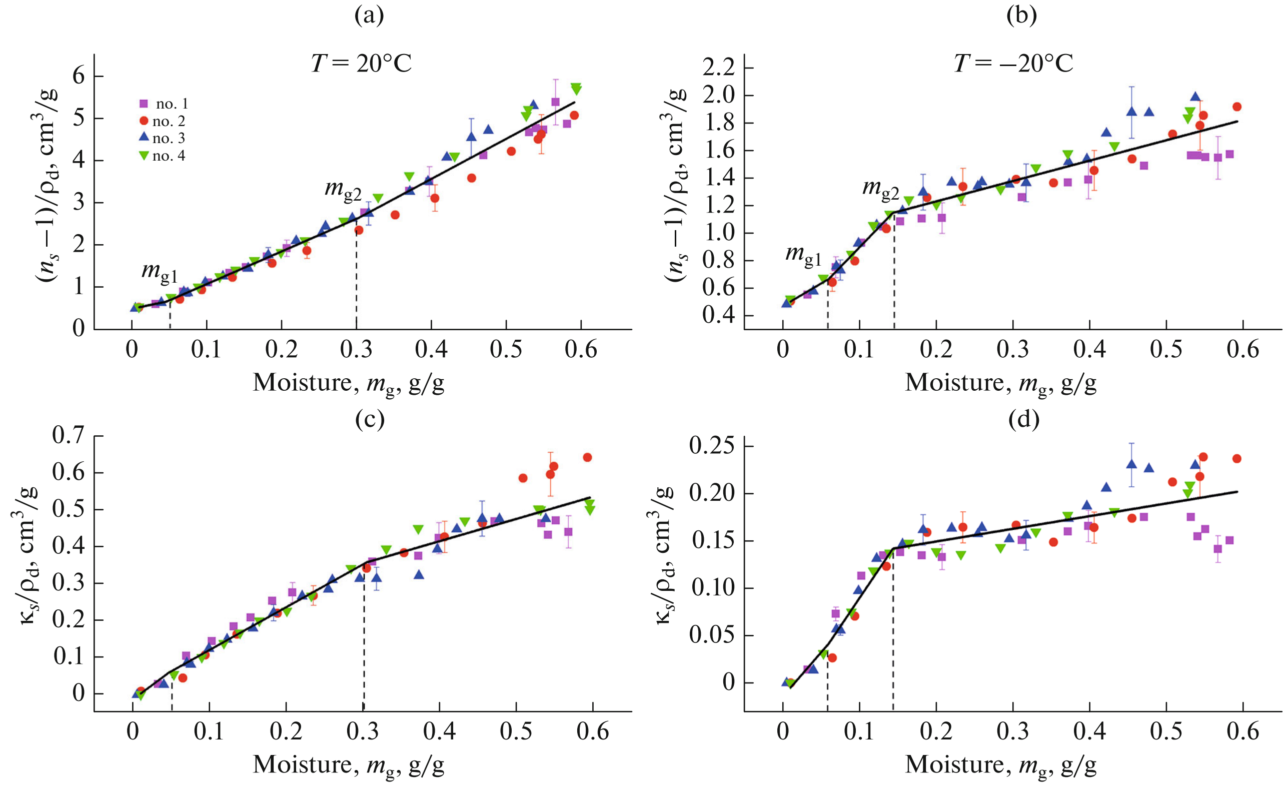

Fig. 2. Reduced RI and NAC of the measured soils at temperatures of (a, c) 20°C and (b, d) −20°C as functions of gravimetric moisture at the frequency of 435 MHz. The experimental data are shown by symbols; the approximation result is shown by lines. The numbers correspond to the numbers of soils from Table 1.

can be seen in Fig. 2, CRI values, depending on moisture, can be indeed described by a piecewise linear function with two breaks. The moisture value m_{g1} determining the first breakpoint of the moisture dependence of the reduced RI and NAC should be referred to boundary moisture separating the moisture ranges related to tightly bound and loosely bound water; the value m_{g2} determining the second breakpoint should be referred to boundary moisture separating the moisture ranges related to loosely bound and unbound water or ice. These ranges are marked in Fig. 2 by vertical dashed lines. Thus, an analysis of the moisture dependences shown in Fig. 2 at the frequency of 435 MHz did not make it possible to separate water bound on the surface of mineral particle and water bound on the surface of organic particles in their dielectric properties for the considered soils. Therefore, all parameters of the dielectric permittivity model that are related to characteristics of bound water categories, like in (Mironov et al., 2010; Mironov and Savin, 2019), will be effective for the whole volume of water bound on mineral and organic particles.

It is seen in Fig. 2 that variations in values of reduced RI and NAC for different soils at similar moistures are small. In regions classified as tightly bound and loosely bound water, values of reduced RI and NAC for different soils almost coincide with each other; in the region of unbound water, they only insignificantly exceed limits of measurement errors for these values. This might indicate that the reduced RI and NAC of the solid component $\left(\frac{n_m - 1}{\rho_m}, \frac{\kappa_m}{\rho_m}\right)$, tightly bound water $\left(\frac{n_b - 1}{\rho_b}, \frac{\kappa_b}{\rho_b}\right)$, loosely bound water $\left(\frac{n_t - 1}{\rho_t}, \frac{\kappa_t}{\rho_t}\right)$, and unbound water (or ice) $\left(\frac{n_{u,i} - 1}{\rho_{u,i}}, \frac{\kappa_{u,i}}{\rho_{u,i}}\right)$, depend weakly or do not depend at all on the organic matter content for the studied soils. Analyzing values of the parameters m_{g1} and m_{g2} for soils with different organic matter content, a weak dependence of m_{g2} on the organic matter content was found at positive temperatures. No such dependence was found at negative temperatures. Taking into account the above, it was decided to exclude from the model the organic matter content as a parameter. Thus, all model parameters described by Eqs. (1) and (2) were common for samples with the organic matter content from 14.8 to 31.1%. As a result of using such approach, the number of parameters of the developed model was reduced, which made it possible to simplify it to some extent.

Parameters of the dielectric model were sought using the procedure of approximation of the obtained moisture dependences of the reduced RI and NAC of

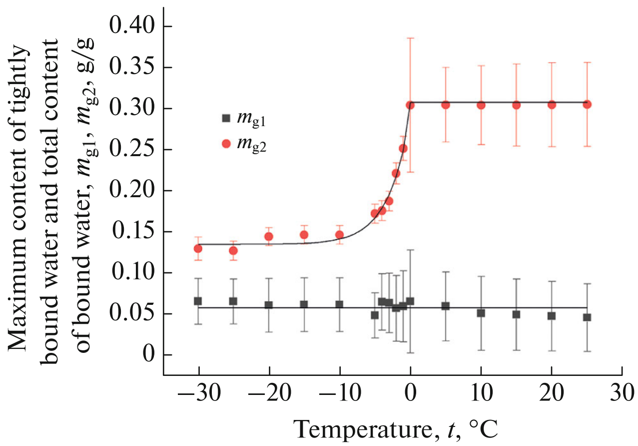

Fig. 3. Maximum content of tightly bound water m_{g1} and total content of bound water m_{g2} in samples of organic soil.

soil samples with the application of formulas (1) and (2) as a theoretical model. In view of the decision not to take into account the organic matter content, the approximation was carried out simultaneously for the RI and NAC of all four studied soils at each measurement temperature. The approximation results are shown in Fig. 2 by solid lines.

Taking into account that the proposed dielectric model was simplified due to the exclusion of the influence of the organic matter content from it; it was necessary to estimate the loss of its accuracy under this assumption. For this purpose, a dielectric model which takes into account the influence of the variation in the organic matter content in the studied soils on the model parameters was constructed. Then, errors in two models of organic soil CDP were analyzed: with allowance for the dependence of CDP model parameters on the organic matter content in the soil and without regard to it. The results of this analysis are presented in the next section.

An approximation of the moisture dependences of the reduced RI and NAC of the soils yielded values of the parameters $\left(\frac{n_m-1}{\rho_m}\right)$, $\left(\frac{\kappa_m}{\rho_m}\right)$, $\left(\frac{n_b-1}{\rho_b}\right)$, $\left(\frac{\kappa_b}{\rho_b}\right)$, $\left(\frac{n_t-1}{\rho_t}\right)$, $\left(\frac{\kappa_t}{\rho_t}\right)$, $\left(\frac{n_{u,i}-1}{\rho_{u,i}}\right)$, $\left(\frac{\kappa_{u,i}}{\rho_{u,i}}\right)$, m_{g1}, and m_{g2} for each temperature from the measurement range, regardless of the organic matter content. Values of the parameters m_{g1} and m_{g2} are shown by symbols in Fig. 3. It is seen in Fig. 3 that m_{g1} within the limits of measurement errors remains a constant equal to 0.06 ± 0.01 g/g in the whole range of measurement temperatures. The quantity m_{g2} slightly varies in the region of positive temperatures and, on average, amounts to 0.31 ± 0.06 g/g. At negative temperatures, the value of m_{g2} decreases with a decrease in temperature by an exponential law from 0.24 to 0.13 g/g.

To describe the temperature dependences of m_{g1} and m_{g2} by use of approximating the experimental data presented in Fig. 3, the following empirical formulas were obtained:

$$m_{g1} = 0.058, \quad -30 \le t \le 25°\text{C},$$
$$m_{g2} = \begin{cases} 0.13 + 0.16\exp(0.32\,t), \\ -30 \le t < 0°\text{C}, \\ 0.307, \quad 0 \le t \le 25°\text{C}. \end{cases} \tag{3}$$

Values of m_{g1} and m_{g2} calculated by formula (3) are shown in Fig. 3 by solid lines.

Applying the approximation method to the obtained moisture dependences of the reduced RI and NAC of the soils under study at each measured temperature with the use of Eqs. (1) and (2) as the theoretical model, temperature dependences were obtained for the parameters characterizing the RI and NAC of the organomineral component, tightly bound water, loosely bound water, unbound water, and ice. The experimental dependences of these parameters are presented in Fig. 4. The following empirical formulas were found by approximation for the experimental temperature dependences:

$$\frac{n_m-1}{\rho_m} = 0.48, \quad \frac{\kappa_m}{\rho_m} = 0.005, \tag{4}$$

$$\frac{n_\text{b}-1}{\rho_\text{b}} = 3.59,$$
$$\frac{\kappa_\text{b}}{\rho_\text{b}} = 0.81 + 0.63e^{0.11t}, \quad -30 \le T < 0°\text{C}, \tag{5}$$
$$\frac{\kappa_\text{b}}{\rho_\text{b}} = 1.34 + 0.01t, \quad 0 \le T \le 25°\text{C},$$

$$\frac{n_\text{t}-1}{\rho_\text{t}} = 7.03 + 0.05t, \quad -30 \le T < 0°\text{C},$$
$$\frac{n_\text{t}-1}{\rho_\text{t}} = 7.68, \quad 0 \le T \le 25°\text{C},$$
$$\frac{\kappa_\text{t}}{\rho_\text{t}} = 0.83 - 0.02t, \quad -30 \le T < 0°\text{C}, \tag{6}$$
$$\frac{\kappa_\text{t}}{\rho_\text{t}} = 0.83 + 0.02t, \quad 0 \le T \le 25°\text{C},$$

$$\frac{n_\text{u}-1}{\rho_\text{u}} = 1.45 + 0.61e^{0.12t}, \quad 30 \le T < 0°\text{C},$$
$$\frac{n_\text{u}-1}{\rho_\text{u}} = 9.93 - 0.02t, \quad 0 \le T \le 25°\text{C},$$
$$\frac{\kappa_\text{u}}{\rho_\text{u}} = 0.14 + 0.09e^{0.19t}, \quad -30 \le T < 0°\text{C}, \tag{7}$$
$$\frac{\kappa_\text{u}}{\rho_\text{u}} = 0.46 + 0.007t, \quad 0 \le T \le 25°\text{C}.$$

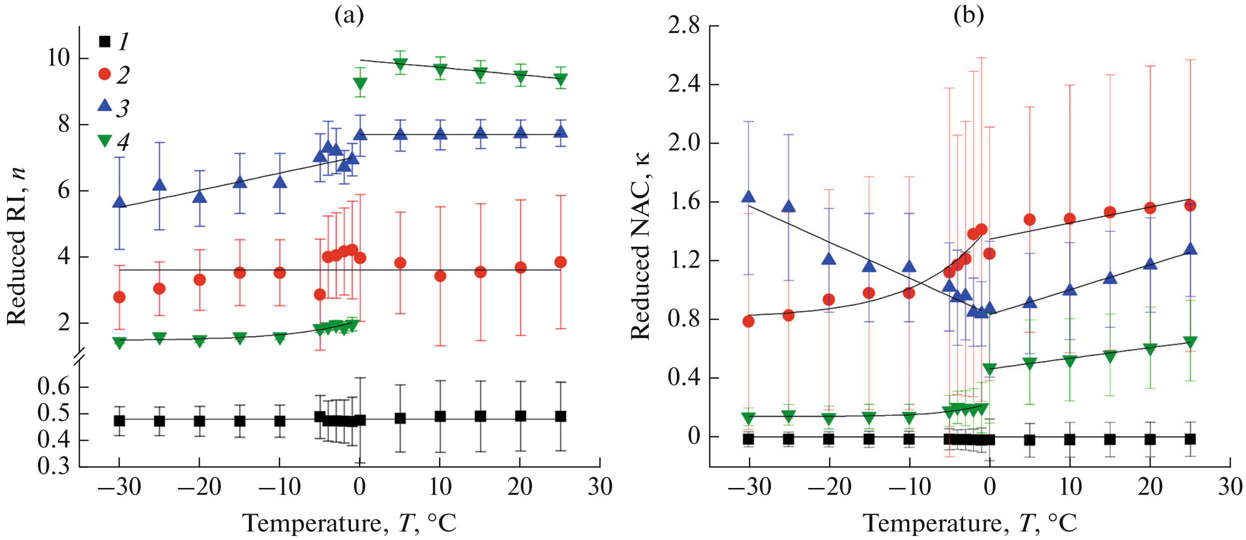

Fig. 4. Temperature dependences of reduced (a) RI n and (b) NAC κ for the (*1*) organomineral component, (*2*) tightly bound water, (*3*) loosely bound water, and (*4*) unbound water (or ice) at the frequency of 435 MHz.

Formulas (1)–(7) constitute the temperature-dependent dielectric model of the upper organic layer of forest soils for the frozen and thawed state at a frequency of 435 MHz. The input parameters of the developed CDP model are the density of dry soil ρ_d, gravimetric moisture content m_g, and temperature t.

In Fig. 4b, one can see that at negative temperatures an increase in the reduced NAC of loosely bound water is observed with a decrease in temperature, while the NAC value decreases for other categories of soil water. Such difference between the NAC temperature dependences of soil water categories in the megahertz frequency range might be caused by the influence of conductivity of soil water categories in combination with relaxation processes related to Maxwell–Wagner interphase polarization (Loewer, 2016; Mironov, 2019). The authors of (Mironov, 2019) revealed two relaxation processes for tightly bound water in organic soils of the Arctic region in the megahertz frequency range; the contribution of these relaxations to the CDP spectrum of tightly bound water decreased with a decrease in temperature in the temperature range from 25 to −30°C and thus decreased the real and imaginary parts of the CRI. Interphase relaxations in organic soil were not revealed in unbound water. In loosely bound water, the maximum absorption frequency of the electromagnetic wave due to Maxwell–Wagner relaxation varied from 1.6 GHz to 280 MHz with a decrease in temperature. At frequencies below the frequency of maximum absorption of the electromagnetic wave due to dielectric relaxation, the NAC increases with a decrease in temperature due to the shift of the absorption maximum to the region of lower frequencies; then, the NAC decreases after the temperature at which the frequency of the electromagnetic field coincides with the maximum absorption frequency. Thus, a change in the maximum absorption frequency of the electromagnetic field due to Maxwell–Wagner relaxation in loosely bound water might lead to a change in the character of the temperature dependence (shown in Fig. 4b) of the reduced NAC of loosely bound water at the frequency of 435 MHz and temperature of about 0°C.

As is seen in Fig. 4b, the values of the reduced NACs of water categories have rather large errors with allowance for the smallness of the values themselves. These errors were calculated as the standard error of parameters obtained in the numerical approximation procedure for moisture dependences (shown in Fig. 2) of the reduced quantities RI and NAC of the soil. The magnitudes of the calculated errors are affected by close values of the NAC of tightly bound and loosely bound water at the frequency of 435 MHz and by the spread of experimental points relative to the theoretical piecewise linear dependence described by formulas (1) and (2). One of causes of the spread of experimental points in Fig. 2 is the error in measurements of the RI and NAC themselves; for the NAC, the relative error is higher by virtue of the fact that its values at the frequency of 435 MHz are considerably less than values of the RI. Other causes are errors in measurements of moisture and density of samples, possible variations in the granulometric and chemical composition in soil samples into which the core was divided.

ESTIMATION OF THE ERROR IN THE DEVELOPED DIELECTRIC MODEL

Errors of the developed single-frequency refractive dielectric model (SFRDM) were estimated by comparing the CDP values calculated using the model with the corresponding measured values. As an example, symbols in Fig. 5 show the measurement results

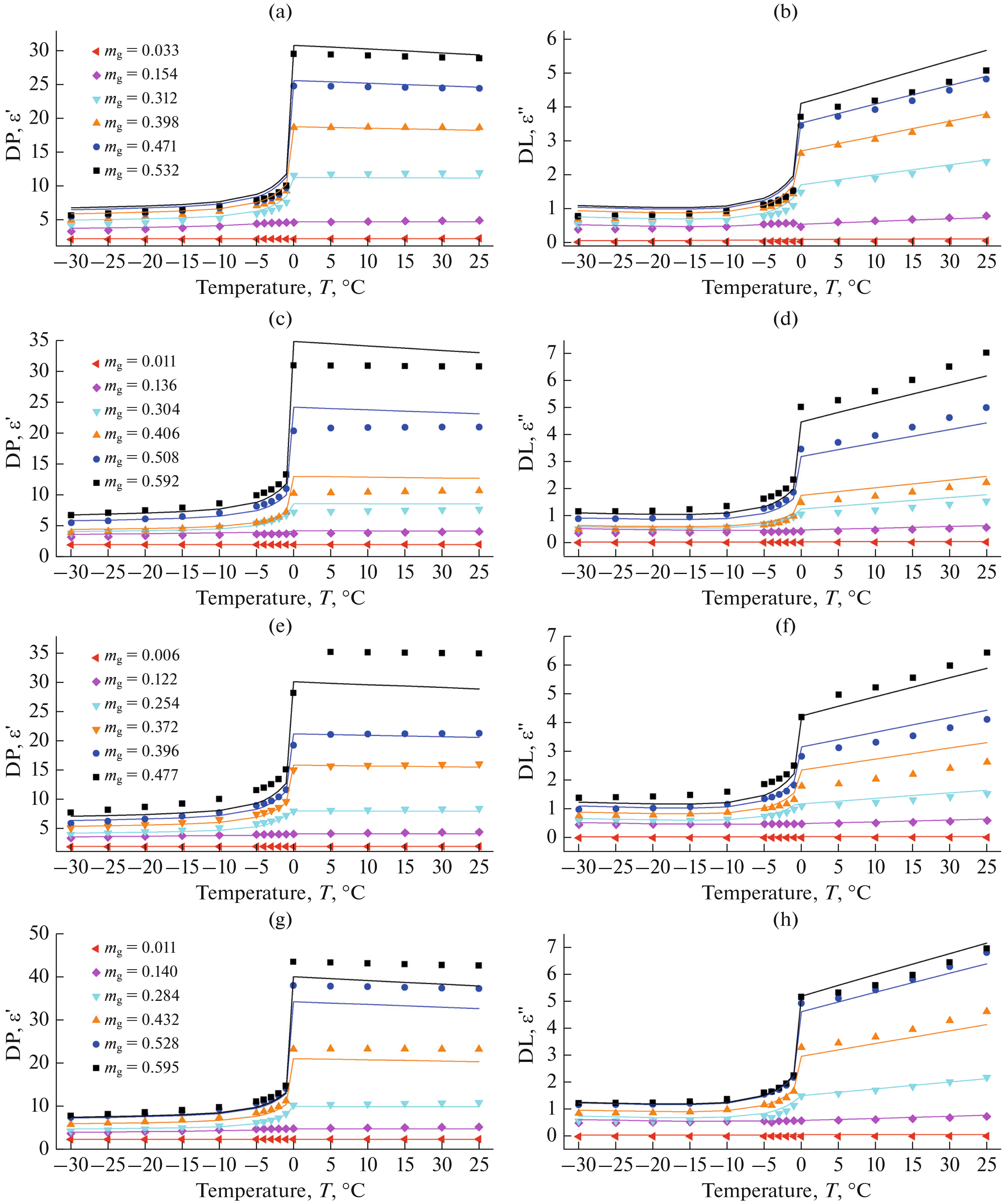

Fig. 5. Values of DP and DL of moist soil samples as functions of temperature: soil no. (a, b) 1, (c, d) 2, (e, f) 3, and (g, h) 4. The measured values are shown by symbols; the solid lines correspond to soil CDP values calculated using the developed model.

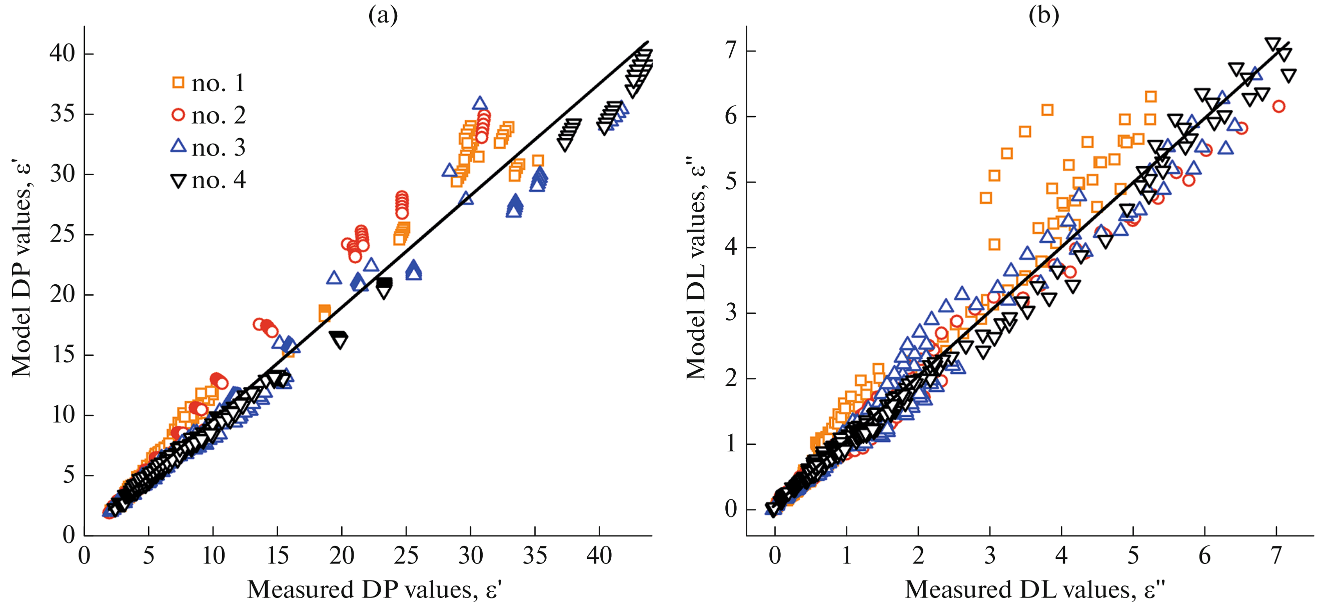

Fig. 6. Values of (a) DP and (b) DL of the studied soils calculated using the developed dielectric model as functions of their measured values. The solid lines show the results of linear approximation.

for DP and DL of four studied soils as functions of temperature for several moistures. Also, solid lines in Fig. 5 show the results of calculations by the proposed dielectric model both for thawed and for frozen states of the upper organic layer of forest soils. As is seen in Fig. 5, a good agreement between the calculated and measured CDP values of moist soils is observed almost in the whole range of measurement temperatures.

Figure 6 shows the DP and DL values for the soils under study calculated using the developed SFRDM as functions of their measured values. To estimate the error of the proposed model of soil CDP for the data presented in Fig. 6, the normalized root-mean-square error (NRMSE) of the model values from measured ones and the coefficient of determination R^2 were calculated. The formulas for calculation of the NRMSE and R^2 have the following form:

$$\mathrm{NRMSE} = \frac{\sqrt{\dfrac{\sum_{j=1}^{n}(x_j - y_j)^2}{n}}}{\bar{x}} \times 100\%, \qquad (8)$$

$$R^2 = 1 - \frac{\sum_j (x_j - y_j)^2}{\sum_j (x_j - \bar{x})^2}, \qquad (9)$$

where x_j, y_j, and $\bar{x}$ are the measured values, values calculated using the model, and the average measured value, respectively; n is the number of measurements. Values of the errors are presented in Table 2. Analyzing the errors presented in Table 2, one may conclude that the accuracy of the proposed model is comparable with the accuracy of CDP measurements.

To estimate the loss of accuracy in the proposed CDP model due to the exclusion of the dependence of the model parameters on the organic matter content in soils from the consideration, the error was also estimated for the single-frequency refractive model of forest soil CDP taking into account variations in the organic matter content in the studied soils (SFRDM OC). Values of the NRMSE and R^2 for the SFRDM OC are also presented in Table 2. Analyzing the data from Table 2, one may conclude that taking into account variations in the organic matter content on parameters of the CDP model does not exert a considerable impact on the accuracy of the model. The difference between the NRMSE values when using the models with allowance for the organic matter content as a model parameter and without regard to it is less than 3% for DP values and less than 1% for DL values. This corroborates the validity of excluding the dependence of parameters of the CDP model for the studied forest soils on the organic matter content in them.

Table 2. Errors of the dielectric models for the studied organic soils

	NRMSE, %		R^2	
	ε'	ε''	ε'	ε''
SFRDM	16	21	0.97	0.97
SFRDM OC	14	22	0.98	0.96

CONCLUSIONS

In this work, a single-frequency dielectric model of thawed and frozen organic forest soils of the root zone at a frequency of 435 MHz is proposed. The model is created based on the refractive dielectric model of the mixture. The developed dielectric model is applicable for predicting CDP of the topsoil of pine, aspen, mixed, and birch forests of Krasnoyarsk forest steppe with an organic matter content from 15 to 31%, gravimetric moisture from 0 to 0.6 g/g, and in the temperature range from −30 to 25°C. In comparison with the spectroscopic dielectric models developed in (Mironov et al., 2020; Mironov and Savin, 2019), the proposed single-frequency model is simpler for practical use, because it has the minimum number of input parameters, which include gravimetric moisture, temperature, and density of dry soil. In the analysis of errors of the created soil CDP model, it has been justified that taking into account the dependence of model parameters on the organic matter content is unnecessary, because the loss of accuracy when excluding this dependence from the consideration, according to the estimation, is less than 3% for DP and less than 1% for DL. The temperature dependence of the maximum possible amount of bound water for the Krasnoyarsk forest-steppe zone has been estimated by the dielectric method for the first time.

This dielectric model can be used for interpreting remote sensing data at a frequency of 435 MHz, as well as in algorithms of moisture measurement and determining the thawed/frozen state of forest soils.

ACKNOWLEDGMENTS

We are grateful to Cand. Sci. (Phys.–Math.) K.V. Muzalevskii, Head of the Laboratory of Remote Sensing Radiophysics, for supporting this work, as well as to I.V. Savin for selecting the studied soil samples.

FUNDING

The study was performed within the framework of the state assignment of the Ministry of Science and Higher Education of Russia, project no. 0287-2021-0034.

CONFLICT OF INTEREST

The authors of this work declare that they have no conflicts of interest.

REFERENCES

Agrokhimicheskie metody issledovaniya pochv (Agrochemical Methods in Soil Research), Sokolov, A.V., Ed., Moscow: Nauka, 1975.

Alemohammad, S.H., Konings, A.G., Jagdhuber, T., Moghaddam, M., and Entekhabi, D., Characterization of vegetation and soil scattering mechanisms across different biomes using P-band SAR polarimetry, *Remote Sens. Environ.*, 2018, vol. 209, pp. 107–117. https://doi.org/10.1016/j.rse.2018.02.032

Belyaeva, T.A., Bobrov, P.P., and Kondrat'eva, O.V., Changes in the dielectric properties of bound water in soil with an increase in its amount, *Vestn. SibGAU*, 2013, no. 5, pp. 92–95.

Bircher, S., Demontoux, F., Zakharova, E, Drusch, M., Wigneron, J.-P., and Kerr, Y.H., L-band relative permittivity of organic soil surface layers: A new dataset of resonant cavity measurements and model evaluation, *Remote Sens.*, 2016, vol. 8, no. 12, p. 1024. https://doi.org/10.3390/rs8121024

Bobrov, P.P., Spectroscopic model of soil dielectric permittivity using standardized agrophysical indicators, *Issled. Zemli Kosmosa*, 2008, no. 1, pp. 15–23.

Bobrov, P.P., Kondrat'eva, O.V., and Mustakova, M.M., Influence of organic matter content in soil on the dielectric permittivity in the frequency range 10–8.5 GHz, *Vestn. SibGAU*, 2013, no. 5, pp. 95–97.

Bobrov, P.P., Belyaeva, T.A., Kroshka, E.S., and Rodionova, O.V., On parameters of the dielectric soil model used in the SMOS algorithm, *Tekh. Radiosvyazi*, 2021, no. 1, pp. 95–102. https://doi.org/10.33286/2075-8693-2021-48-95-102

Bobrov, P.P., Belyaeva, T.A., Kroshka, E.S., and Rodionova, O.V., The effect of dielectric relaxation processes on the complex dielectric permittivity of soils at frequencies from 10 kHz to 8 GHz. Part I: Experimental, *IEEE Trans. Geosci. Remote Sens.*, 2022, vol. 60, pp. 1–9. https://doi.org/10.1109/TGRS.2022.3180727

Boyarskii, D.A. and Tikhonov, V.V., Model of the effective permittivity of wet and frozen soils in the microwave range, *Radiotekh. Elektron.*, 1995, vol. 40, no. 6, pp. 914–917.

Boyarskii, D.A. and Tikhonov, V.V., Effect of bound water on the dielectric permittivity of wet and frozen soils, *Preprint of Space Research Institute, Russ. Acad. Sci.*, Moscow, 2003.

Carreiras, J.M.B., Quegan, S., Le Toan, T., Ho Tong Minh, D., Saatchi, S.S., and Carvalhais, N. Coverage of high biomass forests by the ESA BIOMASS mission under defense restrictions, *Remote Sens. Environ.*, 2017, vol. 196, pp. 154–162. https://doi.org/10.1016/j.rse.2017.05.003

Chudinova, S.M., Dielectric characteristics of soils and categories of soil water, *Eurasian Soil Sci.*, 2009, vol. 42, pp. 405–414. https://doi.org/10.1134/S1064229309040073

Dobson, M., Ulaby, F., Hallikainen, M., and El-Rayes, M., Microwave dielectric behavior of wet soil. Part II: Dielectric mixing models, *IEEE Trans. Geosci. Remote Sens.*, 1985, vol. GE-23, no. 1, pp. 35–46. https://doi.org/10.1109/TGRS.1985.289498

Entekhabi, D., Njoku, E.G., O'Neill, P.E., Kellogg, K.H., Crow, W.T., Edelstein, W.N., Entin, J.K., Goodman, S.D., Jackson, T.J., Johnson, J., Kimball, J., Piepmeier, J.R., Koster, R.D., Martin, N., McDonald, K.C., et al., The Soil Moisture Active Passive (SMAP) mission, *Proc. IEEE*, 2010, vol. 98, no. 5, pp. 704–716. https://doi.org/10.1109/JPROC.2010.2043918

Escorihuela, M.J., Chanzy, A., Wigneron, J.P., and Kerr, Y.H., Effective soil moisture sampling depth of L-band radiometry: A case study, *Remote Sens. Environ.*, 2010, vol. 114, no. 5, pp. 995–1001. https://doi.org/10.1016/j.rse.2009.12.011

Fomin, S.V. and Muzalevskiy, K., Dielectric model for thawed mineral soils at a frequency of 435 MHz, *IEEE Geosci. Remote Sens. Lett.*, 2021, vol. 18, no. 2, pp. 222–225. https://doi.org/10.1109/LGRS.2020.2972559

Garrison, J., Lin, Y.-C., Nold, B., Piepmeier, J.R., Vega, M.A., and Fritts, M., Du Toit, C.F., Knuble, J. Remote sensing of soil moisture using P-band signals of opportunity (SoOp): Initial results, in *2017 IEEE International Geoscience and Remote Sensing Symposium (IGARSS)*, IEEE, 2017, pp. 4158–4161. https://doi.org/10.1109/IGARSS.2017.8127917

Grant, J.P., Van de Griend, A.A., Wigneron, J.-P., Saleh, K., Panciera, R., and Walker, J.P., Influence of forest cover fraction on L-band soil moisture retrievals from heterogeneous pixels using multi-angular observations, *Remote Sens. Environ.*, 2010, vol. 114, no. 5, pp. 1026–1037. https://doi.org/10.1016/j.rse.2009.12.016

Jagdhuber, T., Hajnsek, I., Sauer, S., Papathanassiou, K.P., and Bronstert, A., Soil moisture retrieval under forest using polarimetric decomposition techniques at P-band, in *9th European Conference on Synthetic Aperture Radar*, 2012, pp. 709–712.

Jin, M., Zheng, X., Jiang, T., Li, X., Li, X-J., and Zhao, K., Evaluation and improvement of SMOS and SMAP soil moisture products for soils with high organic matter over a forested area in Northeast China, *Remote Sens.*, 2017, vol. 9, no. 4, p. 387. https://doi.org/10.3390/rs9040387

Kerr, Y.H., Waldteufel, P., Wigneron, J.-P., Delwart, S., Cabot, F., Boutin, J., Escorihuela, M.-J., Font, J., Reul, N., Gruhier, C., Juglea, S.E., Drinkwater, M.R., Hahne, A., Martin-Neira, M., and Mecklenburg, S., The SMOS mission: New tool for monitoring key elements of the global water cycle, *Proc. IEEE*, 2010, vol. 98, no. 5, pp. 666–687. https://doi.org/10.1109/JPROC.2010.2043032

Kochetkova, T.D., Temperature dependence of dielectric permittivity of peat at microwave frequencies, in *8-ya Mezhdunarodnaya nauchno-prakticheskaya konferentsiya "Aktual'nye problemy radiofiziki"* (Proceedings of the 8th International Scientific and Practical Conference "Current Problems of Radiophysics"), 2019, pp. 196–199.

Komarov, A.S. and Mironov, V.L., *Mikrovolnovoye zondirovaniye pochv* (Microwave Sounding of Soils), Novosibirsk: SO RAN, 2000.

Liebmann, P., Wordell-Dietrich, P., Kalbitz, K., Mikutta, R., Kalks, F., Don, A., Woche, S.K., Dsilva, L.R., and Guggenberger, G., Relevance of aboveground litter for soil organic matter formation: A soil profile perspective, *Biogeosciences*, 2020, vol. 17, pp. 3099–3113. https://doi.org/10.5194/bg-17-3099-2020

Liu, J., Zhao, S., Jiang, L., Chai, L., and Wu, F., The influence of organic matter on soil dielectric constant at microwave frequencies (0.5–40 GHz), in *IEEE International Geoscience and Remote Sensing Symposium (IGARSS)*, 2013, pp. 13–16. https://doi.org/10.1109/IGARSS.2013.6721080

Loewer, M., Igel, J., Minnich, C., and Wagner, N., Electrical and dielectric properties of soils in the MHz to GHz frequency range, in *Proceedings of the 11th International Conference on Electromagnetic Wave Interaction with Water and Moist Substances (ISEMA)*, 2016, pp. 247–254.

Mandrygina, V.N., Dielectric permittivity of soils with different humus content and the effect of hydrophobic and hydrophilic pollutants on it, *Extended Abstract of Cand. Sci. (Phys.–Math.) Dissertation*, Omsk Pedagogical University, 2004.

Mironov, V.L. and Savin, I.V., Spectroscopic multirelaxation dielectric model of thawed and frozen Arctic soils considering the dependence on temperature and organic matter content, *Izv., Atmos. Ocean. Phys.*, vol. 55, 2019, no. 9, pp. 986–995. https://doi.org/10.1134/S0001433819090305

Mironov, V.L., Komarov, S.A., Rychkova, N.V., and Kleshchenko, V.N., Study of dielectric properties of wet soils in the microwave range, *Issled. Zemli Kosmosa*, 1994, no. 4, pp. 18–24.

Mironov, V.L., Bobrov, P.P., Bobrov, A.P., Mandrygina, V.N., and Stasuk, V.D., Microwave dielectric spectroscopy of moist soils for a forest-tundra region, in *IEEE International Geoscience and Remote Sensing Symposium*, 2005, pp. 4485–4488. https://doi.org/10.1109/IGARSS.2005.1525917.

Mironov, V.L., De Roo, R.D., and Savin, I.V., Temperature-dependable microwave dielectric model for an Arctic soil, *IEEE Trans. Geosci. Remote Sens.*, 2010, vol. 48, no. 6, pp. 2544–2556. https://doi.org/10.1109/TGRS.2010.2040034

Mironov, V.L., Bobrov, P.P., and Fomin, S.V., Multirelaxation generalized refractive mixing dielectric model of moist soils, *IEEE Geosci. Remote Sens. Lett.*, 2013a, vol. 10, no. 3, pp. 603–606. https://doi.org/10.1109/LGRS.2012.2215574

Mironov, V.L., Molostov, I.P., Lukin, Y.I., and Karavaisky, A.Y., Method of retrieving permittivity from S12 element of the waveguide scattering matrix, in *2013 International Siberian Conference on Control and Communications (SIBCON)*, IEEE, 2013b, pp. 1–3. https://doi.org/10.1109/SIBCON.2013.6693609.

Mironov, V.L., Karavayskiy, A.Y., Lukin, Y.I., and Molostov, I.P., A dielectric model of thawed and frozen Arctic soils considering frequency, temperature, texture and dry density, *Int. J. Remote Sens.*, 2020, vol. 41, no. 10, pp. 3845–3865. https://doi.org/10.1080/01431161.2019.1708506

Monerris, A., Vall-llossera, M., Camps, A., Sabia, R., Villarino, R., Cardona, M., Alvarez, E., and Sosa, S., Soil moisture retrieval using L-band radiometry: Dependence on soil type and moisture profiles, in *2006 MicriRad*, IEEE, 2006, pp. 171–175. https://doi.org/10.1109/MICRAD.2006.1677083

Muzalevskii, K.V., The potential of remote sensing of soil moisture profile based on backscattering polarimetric observations in P- and C-bands, *Sovrem. Probl. Distan-*

tsionnogo Zondirovaniya Zemli Kosmosa, 2019, vol. 16, no. 5, pp. 203–216.

Nagarajan, K., Judge, J., Monsivais-Huertero, A., and Graham, W.D., Impact of assimilating passive microwave observations on root-zone soil moisture under dynamic vegetation conditions, *IEEE Trans. Geosci. Remote Sens.*, 2012, vol. 50, no. 11, pp. 4279–4291. https://doi.org/10.1109/TGRS.2012.2191154

Owe, M. and Van de Friend, A., Comparison of soil moisture penetration depths for several bare soils at two microwave frequencies and implications for remote sensing, *Water Resour. Res.*, 1998, vol. 34, no. 9, pp. 2319–2327.

Pan, M., Sahoo, A.K., Wood, E.F., Al Bitar, A., Leroux, D., and Kerr, Y.H., An initial assessment of SMOS derived soil moisture over the continental United States, *IEEE J. Sel. Top. Appl. Earth Obs. Remote Sens.*, 2012, vol. 5, no. 5, pp. 1448–1457. https://doi.org/10.1109/JSTARS.2012.2194477

Pan, M., Cai, X., Chaney, N.W., Entekhabi, D., and Wood, E.F., An initial assessment of SMAP soil moisture retrievals using high-resolution model simulations and in situ observations, *Geophys. Res. Lett.*, 2016, vol. 43, no. 18, pp. 9662–9668. https://doi.org/10.1002/2016GL069964

Park, C.-H., Behrendt, A., LeDrew, E., and Wulfmeyer, V., New approach for calculating the effective dielectric constant of the moist soil for microwaves, *Remote Sens.*, 2017, vol. 9, p. 732. https://doi.org/10.3390/rs9070732

Park, C.-H., Montzka, C., Jagdhuber, T., Jonard, F., De Lannoy, G., Hong, J., Jackson, T.J., and Wulfmeyer, V., A dielectric mixing model accounting for soil organic matter, *Vadose Zone J.*, 2019, vol. 18, p. 190036. https://doi.org/10.2136/vzj2019.04.0036

Patil, C.B. and Chaudhari, P.R., Dielectric constant and emissivity of forest soil samples at microwave frequency, *Int. J. Sci. Res. Phys. Appl. Sci.*, 2018, vol. 6, no. 4, pp. 44–46. https://doi.org/10.26438/ijsrpas/v6i4.4446

Peplinski, N.R., Ulaby, F.T., and Dobson, M.C., Dielectric properties of soils in the 0.3–1.3 GHz range, *IEEE Trans. Geosci. Remote Sens.*, 1995, vol. 33, no. 3, pp. 803–807. https://doi.org/10.1109/36.387598

Reigber, A., Jager, M., Pinheiro, M., Scheiber, R., Prats, P., Fischer, J., Horn, R., and Nottensteiner, A., Performance of the P-band subsystem and the X-band interferometer of the F-SAR airborne SAR instrument, in *2012 IEEE International Geoscience and Remote Sensing Symposium*, IEEE, 2012, pp. 5037–5040. https://doi.org/10.1109/IGARSS.2012.6352479.

Repin, A.V., Methods for measuring the dielectric permittivity of various types of soil moisture and oil-bearing rocks, *Extended Abstract of Cand. Sci. (Phys.–Math.) Dissertation*, Omsk State Pedagogical University, 2010.

Sadeghi, M., Tabatabaeenejad, A., Tuller, M., Moghaddam, M., and Jones, S., Advancing NASA's AirMOSS P-band radar root zone soil moisture retrieval algorithm via incorporation of Richards' equation, *Remote Sens.*, 2016, vol. 9, no. 1, p. 17. https://doi.org/10.3390/rs9010017

Savin, I.V., Muzalevskiy, K.V., and Mironov, V.L., A dielectric model of thawed and frozen Arctic organic soils at 435 MHz, *Remote Sens. Lett.*, 2022, vol. 13, no. 5, pp. 452–459. https://doi.org/10.1080/2150704X.2022.2041761

Shen, X., Walker, J.P., Ye, N., Wu, X., Boopathi, N., Yeo, I.-Y., Zhang, L., and Zhu, L., Soil moisture retrieval depth of P- and L-band radiometry: Predictions and observations, *IEEE Trans. Geosci. Remote Sens.*, 2021, vol. 59, no. 8, pp. 6814–6822. https://doi.org/10.1109/TGRS.2020.3026384

Shukla, J. and Mintz, Y., Influence of land-surface evapotranspiration on the Earth's climate, *Science*, 1982, vol. 215, no. 4529, pp. 1498–1501. https://doi.org/10.1126/science.215.4539.1498

Shutko, A.M., *SVCh-radiometriya vodnoi poverkhnosti i pochvogruntov* (Microwave Radiometry of Water Surface and Soils), Nauka, 1986.

Szypłowska, A., Lewandowski, A., Yagihara, S., Saito, H., Furuhata, K., Szerement, J., Kafarski, M., Wilczek, A., Majcher, J., Woszczyk, A., and Skierucha, W., Dielectric models for moisture determination of soils with variable organic matter content, *Geoderma*, 2021, vol. 401, p. 115288. https://doi.org/10.1016/j.geoderma.2021.115288

Tabatabaeenejad, A., Burgin, M., Xueyang, Duan., and Moghaddam, M., P-band radar retrieval of subsurface soil moisture profile as a second-order polynomial: First AirMOSS results, *IEEE Trans. Geosci. Remote Sens.*, 2015, vol. 53, no. 2, pp. 645–658. https://doi.org/10.1109/TGRS.2014.2326839

Wang, J.R. and Schmugge, T.J., An empirical model for the complex dielectric permittivity of soils as a function of water content, *IEEE Trans. Geosci. Remote Sens.*, 1980, vol. GE-18, no. 4, pp. 288–295. https://doi.org/10.1109/TGRS.1980.350304

Ye, N., Walker, J.P., Yeo, I.-Y., Jackson, T.J., Kerr, Y., Kim, E., Mcgrath, A., Popstefanija, I., Goodberlet, M., and Hills, J., Toward P-band passive microwave sensing of soil moisture, *IEEE Geosci. Remote Sens. Lett.*, 2020, vol. 18, no. 3, pp. 504–508. https://doi.org/10.1109/LGRS.2020.2976204

Zhang, L., Zhao, T., Jiang, L., and Zhao, S., Estimate of phase transition water content in freeze-thaw process using microwave radiometer, *IEEE Trans. Geosci. Remote Sens.*, 2010, vol. 48, no. 12, pp. 4248–4255. https://doi.org/10.1109/TGRS.2010.2051158

Zhang, N., Shi, J., Sun, G., Guo, Z., and Chai, L., Assessment of boreal forest biomass using L-band radiometer SMOS data, in *2011 IEEE International Geoscience and Remote Sensing Symposium*, 2011, pp. 1946–1949. https://doi.org/10.1109/IGARSS.2011.6049507

Translated by A. Nikol'ski

Publisher's Note. Pleiades Publishing remains neutral with regard to jurisdictional claims in published maps and institutional affiliations.